UNSUPERVISED VARIATIONAL CLASSIFICATION THROUGH IMAGE MULTI-THRESHOLDING

L. Klaine, B. Vozel, K. Chehdi

IETR, UMR CNRS 6164 - University of RENNES I,
BP 80518 - 22305 Lannion Cedex - FRANCE

ABSTRACT

In this paper, we propose an improvement of the classical image multi-thresholding methods. The goal is to achieve the precise determination of homogeneous zones in numerical images by pixels classification. The thresholds and the modes are obtained by minimization of a new energy of gravitational clustering initialized with the significant peaks of a cumulated histogram. Then, the best modes and the best thresholds are calculated by alternate optimization of an energy of multi-thresholding, leading to a piecewise quadratic potential. This energy is built from a total uniformity criterion which measures the homogeneity of a given map of regions. Finally, an unsupervised classification is performed by use of a supervised variational classification approach which minimizes an adapted energy of transitions of phases. The potential which controls the classification process is built from the previously determined best thresholds and modes. The experimental study shows the efficiency and the robustness of the whole method.

1. INTRODUCTION

This paper is devoted to the problem of the precise determination of homogeneous zones in numerical images by pixels classification. We propose an improvement of classical multi-thresholding methods.

The proposed method is composed of four steps. The gravitational step gives a first determination of the significant thresholds and modes of the processed image. From the representation of its histogram in the form of a dynamic system, it is shown that the final histogram converges towards a multimodal histogram. The method is optimal and minimizes a specific energy denoted *e*nergy of gravitational clustering. The subsequent multi-thresholding step performs the determination of the best thresholds and the best modes with regard to the total uniformity criterion. The proposed algorithm is optimal and minimizes an energy called *multi-thresholding energy*. The final unsupervised classification makes use of the supervised classification method by variational approach of [7], [2, 1]. The potential which controls the algorithm is completely determined by the previously obtained best thresholds and modes. The experimental study is carried out in the last section on different degraded images to show the efficiency and the robustness of the whole method.

This work was supported by the Regional Council of Brittany , and the ERDF through the european Interreg3b project

2. FIRST STEP : GRAVITATIONAL CLUSTERING

2.1. Motivations

An histogram can be viewed as multimodal if the modes are sufficiently distant from each other. However, the multi-modality is not well defined as the minimal distance between the modes is not explicitly given.

The histogram transformation that we propose, considers an alternative modelling of the histogram by a dynamic representation. The values of the histogram are comparable with the masses and the samples with the positions of a dynamic system of the previously defined masses.

The gravitational clustering does not apply to the histogram itself but to its dynamic representation. The previous multi-modality point of view is then translated to the positions vectors. It is expressed using the distance between two components of the positions vectors rather than by using a distance between the values of the original histogram.

Formally, we allow the histogram to take real values but only in the range of real light intensities I. It must be contained in $C(I)$ the closed convex envelope of I.

In other words, the histograms are in $\mathcal{H}_I^+(c(I))$ where $\mathcal{H}_a^+(b)$ denotes the set of *histograms indexed on* A *with support in* B if $A \neq B$. A dynamic *system* on I is a two-uplet $(\vec{h};\vec{x}) \in \mathbb{R}^I \times \mathbb{R}^I$ of vectors indexed on I. The mobile vector $\vec{x}$ is called the *vector of the positions*, the fixed vector $\vec{h}$ is called the *vector of the masses*.

The initial vector of the positions $\vec{x}^0$ is defined by $x_i^0 = i$. The vector of the masses $\vec{h}$ is defined by $\vec{h} = \vec{h}^{\text{cum}}$ where $h_i^{\text{cum}} = \mu^{\text{cum}}(\{i\})$. h_i^{cum} are the significant peaks of the cumulated histogram $\vec{h}^{\text{cum}}$. They are computed from local histograms computed on sliding windows with different sizes (16×16, 32×32, 64×64) of the original image. The different sizes of the sliding window allow to take account of the spatial resolution of the image and to get an initial histogram $\vec{x}^0$ with a well pronounced multi-modal form [5].

The gravitational clustering acts by moving the positions vector of the initial vector given by $\vec{x}^0$. Its trajectory is modelled by a function $\vec{x}(\cdot) : \mathbb{R}^+ \mapsto C(I)^I$ such as $\vec{x}(0) = \vec{x}^0$.

2.2. The Gravitational Energy

The energy of gravitational clustering is defined by:

$$Q_{\text{gc}}(\vec{h};\vec{x}) \triangleq \frac{1}{2}\sum_{i\in I}\sum_{j\in I} h_i h_j \delta_{i,j}(\vec{x})|x_i - x_j|^2 \tag{1}$$

It measures the dispersion of the positions with regard to the relative centres of gravity. We call *centre of gravity* relative to a position, the barycentre of the positions located within a radius lower than a maximum preset distance and named *gravitational radius*. The gravitational radius is a C^1 function on the set of the positions $C(I)$ and with value in a compact of $\mathbb{R}^{*+}$. Thus, the maximum distance is not constant, it is a function of the position of the considered masses.

The gravitational equation is built to cancel the derivative of the energy of gravitational clustering $\vec{x}$ minimize $Q_{\mathrm{gc}}(\vec{h};\vec{x})$. This equation defines the trajectory of the positions through the gravitational field.

$$\vec{x}(0)=\vec{x}^0 \text{ and } \frac{\mathrm{d}\vec{x}}{\mathrm{d}t}(t)=\vec{G}(\vec{h};\vec{x}(t))-\vec{x}(t)$$

$$t\rightarrow+\infty$$

Each position can be moved towards its relative centre of gravity. $\vec{x}=\vec{G}(\vec{h};\vec{x})$ where the gravitational field is given by:

$$\vec{G}(\vec{h};\vec{x}) \triangleq \mathbf{G}(\vec{h};\vec{x}).\vec{x} \quad (2)$$

$$G_{i,j}(\vec{h};\vec{x}) \triangleq \left[\sum_{k\in I}\delta_{i,k}(\vec{x})h_k\right]^{-1}\delta_{i,j}(\vec{x})h_j \quad (3)$$

$$\delta_{i,j}(\vec{x}) \triangleq H(R(x_i,x_j)-|x_i-x_j|) \quad (4)$$

The condition $R(x_i,x_j)=\sup(R(x_i),R(x_j))>|x_i-x_j|$ simply translate the determination of the relative centres of gravity.

The trajectory is simply controlled by the proximity and the importance of specific masses. The positions are attracted by their relative centres of gravity. The gravitational radius is essential to precisely quantify the multi-modality with regard to the positions of the modes.

In an initial version of the method, the relative centre of gravity is calculated starting from the positions located in a constant radius R_0. In an improved version of the method, we authorize the radius $R(\cdot)$ to be contrast dependent.

We consider a vector of the positions as multimodal if and only if it merges with the vector of the relative centres of gravity.

Regular approximation of the gravitational field is then considered. It has exactly the same properties as those of the gravitational field. The regularity of the gravitational ε-regularized field directly ensures the existence and the uniqueness of a maximum solution on $\mathbb{R}^+$ thanks to the theorem of Cauchy-Lipschitz.

2.3. Implementation

The trajectory of the vector of the positions cannot be calculated from the exact solving of its evolution ε-regularized equation. In practice, the gravitational processing of an histogram can only be carried out using a discrete algorithm. The solution is modelled by the following gravitational ε-regularized continuation. It is obtained using an explicit numerical scheme. by simple discretization of the gravitational ε-regularized equation using the finite differences:

$$\vec{x}^{n+1}=\vec{x}^n+\Delta t\Big[\vec{G}(\vec{h},\varepsilon;\vec{x}^n)-\vec{x}^n\Big] \quad (5)$$

$$=\Big[\Delta t.\mathbf{G}(\vec{h},\varepsilon;\vec{x}^n)+(1-\Delta t).\mathbf{Id}\Big].\vec{x}^n \quad (6)$$

The recurrence formula is repeated until the vector $\vec{g}(\vec{h}^{\mathrm{cum}};\vec{x}^n)$ is stable by the gravitational ε-regularized field. The vector is *strongly multimodal* , it satisfies $G_i(\vec{h}^{\mathrm{cum}};\vec{x}^n)=G_j(\vec{h}^{\mathrm{cum}};\vec{x}^n)$ if $\delta_{i,j}(\vec{g}(\vec{h}^{\mathrm{cum}};\vec{x}^n))=1$.

We have shown that the vector satisfying this condition is actually reached in a finite number of iteration. Moreover, its image by the gravitational field merge with the vector of the centres of gravity obtained at convergence.

Thus, the gravitational clustering returns a vector of the positions gradually constant on each class. Visually, the vector of the positions takes a staircase shape.

The positions are converted into integer values to preserve a meaning in the set of light intensities.

The histogram corresponding to $\vec{x}^\infty$ is denoted histogram of the centres of gravity $h^{\mathrm{gc}}(\cdot)$. It is multimodal and the modes are given by the various levels of the vector $\vec{x}^\infty$.

For this reason, we decide to stop the algorithm as soon as $d(G_i(\vec{h}^{\mathrm{cum}};\vec{x}^n))=d(G_j(\vec{h}^{\mathrm{cum}};\vec{x}^n))$ if $\delta_{i,j}(\vec{g}(\vec{h}^{\mathrm{cum}};\vec{x}^n))=1$.

This corresponds to *weak multi-modality* as opposed to *strong multi-modality*.

3. SECOND STEP : THE MULTI-THRESHOLDING ENERGY

The thresholds define a partition of the set of the light intensities. The classes are formed of the intervals ranging between two consecutive thresholds. The modes are point to point associated with the classes. They provide each one a single characteristic value of the class. We deduce from it that the thresholds and the modes must be ordered so that each mode lies between two consecutive thresholds.

The aim of this section is to determine the best thresholds and the best modes with regard to a criterion denoted *the total uniformity criterion*. This choice is not coarse and the most intuitive is not necessarily the best.

The *total uniformity criterion* measures the quality of a map of homogeneous areas. Its principle is built on the idea that an area is *uniform* if the dispersion of the grey levels is weak.

We can measure the uniformity of an area by estimating the *intra-area variance*. A map of areas is known as uniform if the areas which make it up, are uniform. We estimate the *total uniformity* of a map by the weighted average, by the size of the different areas, of the intra-area variances.

$$\begin{aligned}\mathrm{TU}(u;u_h) &\triangleq \sum_{k=1}^{N} N_k(h;\vec{s})V_k(h;\vec{s})\\ &\triangleq \sum_{k=1}^{N}\int_{s_{k-1}}^{s_k} h(t)\big|t-M_k(h;\vec{s})\big|^2\mathrm{d}t\end{aligned} \quad (7)$$

where

$$M_k(h;\vec{s}) \triangleq \left[\int_{s_{k-1}}^{s_k} h(t)\mathrm{d}t\right]^{-1}\int_{s_{k-1}}^{s_k} th(t)\mathrm{d}t \quad (8)$$

and $\{u_h=l\}$ is the area of label l.We expect the procedure of extraction of the best thresholds and the best modes to minimize this total uniformity criterion. Unfortunately, the formulation of this criterion does not depend on neither the thresholds nor the modes. The energy of multi-thresholding is built in order to coincide exactly with the total uniformity if the modes are equal to the intra-area means. It measures the quality of the modes and the thresholds knowing their number. This quality is estimated by regarding the vector of the thresholds as an approximation in N samples of the histogram. Its discrete version is given by:

$$
\begin{aligned}
Q_{\mathrm{mt}}(h;\vec{s},\vec{m}) \triangleq\ & \frac{1}{2}\sum_{k=0}^{N}\ \sum_{x_j>s_k}^{x_j<s_{k+1}} h_j|x_j-m_k|^2 \\
& +\frac{1}{2}\sum_{k=1}^{N-1}\ \sum_{x_j=s_k} h_j \min\left(|x_j-m_k|^2, |x_j-m_{k+1}|^2\right)
\end{aligned} \tag{9}
$$

The optimal solution consists of a continuation which alternatively minimizes the multi-thresholding energy with regard to the modes and the thresholds. Assuming the modes $\vec{m}$ known, the energy of multi-thresholding $Q_{\mathrm{mt}}(h;\vec{s},.)$ is convex with respect to the thresholds. It admits a single minimum. This one is simply given by the middle of the interval ranging between two modes:

$$
s_k^n = \left(m_k^n + m_{k+1}^n\right)/2 \tag{10}
$$

Assuming the thresholds $\vec{s}$ known, the vector of the modes which minimizes the multi-thresholding energy is given by the barycentres of the thresholds whose weights depend on the thresholds and the histogram:

$$
m_k^{n+1} = M_k(h;\vec{s}^n) \tag{11}
$$

The obtained solution at convergence $(\vec{s}^m t, \vec{m}^m t) = \lim(\vec{s}^n, \vec{m}^n)$ corresponds then to the best classification, since the multi-thresholding energy limits to the maximum the error with the initial distribution of the masses.

When the image is slightly degraded, the analysis of the histogram does not make it possible to correctly extract the modes and the thresholds. It depends on the relative value of the noise standard deviation from the inter-area contrast value. The use of an isotropic filter of the heat equation type adapted to the noise standard deviation value[6] allows to reveal the modes. Moreover, the filter does not only regularize the image but the histogram too.

4. CLASSIFICATION

When the image is seriously degraded, the previous filtering pretreatment is not more sufficient and it is necessary to consider an *a priori* homogeneity constraint to improve the classification result. Now, the problem is to find a classification method to which it would be sufficient to give a set of representative modes of the classes and which could take into account such an *a priori* homogeneity constraint. The modes would be given by the results of the previously described multi-thresholding second step, leading necessarily to a supervised classification method. Such a method exists in the variational framework. The *a priori* homogeneity constraint can be introduced by adding to the usual classification term, defined by a potential, an additional regularization term translating the homogeneity constraint. This method was developed by Samson [7] and then Aubert and *al* [2, 1]. It derives from the various work undertaken on the theory of Van der Waals-Cahn-Hilliard in mechanics of fluids for the phases transitions [3, 4, 8].

The efficacy of image classification by the variational approach generally depends on the relevant choice of the involved parameters such as the potential $W(\cdot)$. The potential $W(\cdot)$ is completely determined by its stable and unstable phases.

$$
Q_{\mathrm{pt}}(W;u) \triangleq \int_{\Omega} W(u) \tag{12}
$$

In our work, this classification method becomes attractively unsupervised since the potential is automatically given from the best thresholds $\vec{s}^{mt}$ and the best modes $\vec{m}^{mt}$. It is sufficient for that to build a potential whose stable phases are given by the modes. The unstable phases are then given by the thresholds. We define the potential $W(\vec{s},\vec{m};\cdot) : \mathbb{R} \mapsto \mathbb{R}^+$ by:

$$
W(\vec{s},\vec{m};U) \triangleq \begin{cases}
+|U-m_1|^2/|m_1-s_1|^2 & \text{if } U \in]-\infty, s_1-\eta[, \\
+|U-m_k|^2/|m_k-s_{k-1}|^2 & \text{if } U \in]s_{k-1}+\eta, m_k-\eta[, \\
-|U-s_k|^2/|s_k-m_k|^2 + A_k(\eta) & \text{if } U \in]s_k-\eta, s_k+\eta[, \\
+|U-m_k|^2/|s_k-m_k|^2 & \text{if } U \in]m_k+\eta, s_k-\eta[, \\
+|U-m_N|^2/|m_N-s_{N-1}|^2 & \text{if } U \in]s_{N-1}+\eta, +\infty[.
\end{cases} \tag{13}
$$

with $A_k(\eta) \triangleq 1 - 2\eta/|s_k-m_k| + 2\eta^2/|s_k-m_k|^2$ to get a sufficiently regular potential. In practice, the value of η is taken very near or equal to zero. Then, Q_{pt} writes:

$$
Q_{\mathrm{pt}}(W,\varphi,\varepsilon;u) \triangleq \int_{\Omega}\left[\varepsilon\varphi(|\nabla u|) + \frac{1}{\varepsilon}W(u)\right] \tag{14}
$$

Two different schemes can be considered to get the solution. A first scheme performs an alternate minimization using the semi-quadratic algorithm [7] and [2, 1]. The second scheme realizes a direct minimization of the dynamic equation associated with (14) [7] and [2, 1]. However, the method of alternate minimization is more precise than that of the direct resolution of the dynamic equation when the regularization parameter is suitably selected.

5. EXPERIMENTAL RESULTS

The comparative study was carried out by first applying the initial and improved gravitational methods on different images of the french data bank of the GDR-PRC-ISIS, among them [LENA], [BATEAU] and [SAVOISE]. The number of modes was initially obtained by the initial method. The amplitude of the gravitational radius was then modulated in the improved method in order to obtain the same number of modes. We retain the *total uniformity* criterion as the main evaluation criterion. We also consider the usual comparison criteria of two images: the mean absolute error MAE, the mean quadratic error MQE, the maximum error ME, the peak signal-to-noise ratio $PSNR$. The objective is to prove the homogeneity of the areas composing a given image. The quality of the images obtained by the improved method is globally more homogeneous than that of the images obtained by the initial method (Fig.1).

Algorithme	TU	Comparative Criteria			
		[MAE]	[MSE]	[ME]	[PSNR$_{\mathrm{dB}}$]
Initial Method	42.783	5.966	7.067	**25**	31.146
Improved Method	**33.757**	**4.904**	**5.818**	30	**32.836**
Initial Method	56.069	6.358	7.683	39	30.420
Improved Method	**51.944**	**6.122**	**7.211**	**36**	**30.971**
Initial Method	**4.252**	**0.426**	**2.126**	**90**	**41.581**
Improved Method	**4.252**	**0.426**	**2.126**	**90**	**41.581**

Table 1. Comparative results of the initial and improved methods, up and down for the images [BATEAU] 10 modes, [LENA] 8 modes, and [SAVOISE] 3 modes

Table 1 confirms the visual observation of the processed images: the results are generally better for the improved method, except for the maximum error criterion. Indeed, the improved method can lead to a punctual large deviation of light intensity between the original image and the multi-thresholded image if this deviation are compensated on the overall image.

Now, to prove the robustness to the observation noise, the three images were preliminary degraded with additive noise (2). Three methods of determination of homogeneous zones are subsequently compared: a multi-thresholding method previously developed by the authors [Kerm], the direct minimization [Sams^1] and finally the alternate minimization [Sams^2] [7] and [1].

We present afterwards the original image [LENA], the degraded image, the potential used to control the classification, as well as the obtained map of homogeneous areas (Fig.2).

In order to objectively evaluate the results, we estimate the total uniformity measure on the original images using each obtained map of homogeneous areas.

Image		[Kerm]	[Sams^1]	[Sams^2]
[BATEAU]	$\sigma_b = 12$	221.749	128.653	**115.039**
[LENA]	$\sigma_b = 10$	169.899	**126.72**	133.652
[SAVOISE]	$\sigma_b = 14$	248.378	**211.116**	213.658

Table 2. Total Uniformity

The method of classification using the alternate minimization is better provided that the parameter of regularization is well selected. However, it is much slower and more constraining than the method using direct minimization. The results obtained by the latter are quite good and easier to control.

6. SUMMARY AND CONCLUSIONS

Classification of degraded images with different noise levels show the potential of the whole system: it is rather effective for the determination of homogeneous areas in an image, and allows a significant data reduction.

The proposed method has the main advantage to be optimal and robust to the observation noise. The results can be easily used for further image processing tasks: for example, to identify the nature of the noise and to estimate its variance.

7. REFERENCES

[1] G. Aubert, L. Blanc-Féraud, and R. March. Γ-convergence of discrete functionals with non-convex perturbation for image classification. Technical Report 4560, Institut National de Recherche en Informatique et en Automatique, September 2002.

[2] G. Aubert and P. Kornpobst. *Mathematical problems in image processing (Partial differential equations and the calculus of variations)*. Springer, 2002.

[3] J. Cahn and J.E. Hilliard. Free energy of a nonuniform system i. interfacial free energy. *Journal of chemical physics*, 28(1):258–267, 1958.

[4] I. Fonseca and L. Tartar. The gradient theory of phase transitions for systems with two potential wells. *Proc. R. Soc. Edinb., Sect.*, 111(A-1/2):89–102, 1989.

[5] C. Kermad and K. Chehdi. Research of an automatic and unsupervised system of segmentation. *Image and Vision Computing, Edition Elsevier*, pages 541–555, 2002.

[6] J.J. Koenderink. The structure of images. *Biological Cybernetics*, 50:363–370, 1984.

[7] C. Samson, L. Blanc-Féraud, G. Aubert, and J. Zerubia. A variational model for image classification and restoration. *IEEE Transaction on Pattern Analysis and Machine Intelligence*, 22(5):460–472, May 2000.

[8] P. Sternberg. Vector-valued local minimizers of non-convex variational problems. *Rocky Mt. J. Math*, 21(2):799–807, 1991.

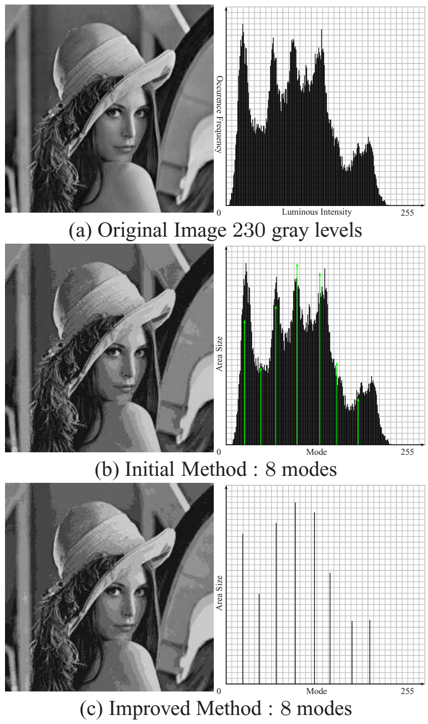

(a) Original Image 230 gray levels

(b) Initial Method : 8 modes

(c) Improved Method : 8 modes

Fig. 1. Homogeneous areas [LENA]

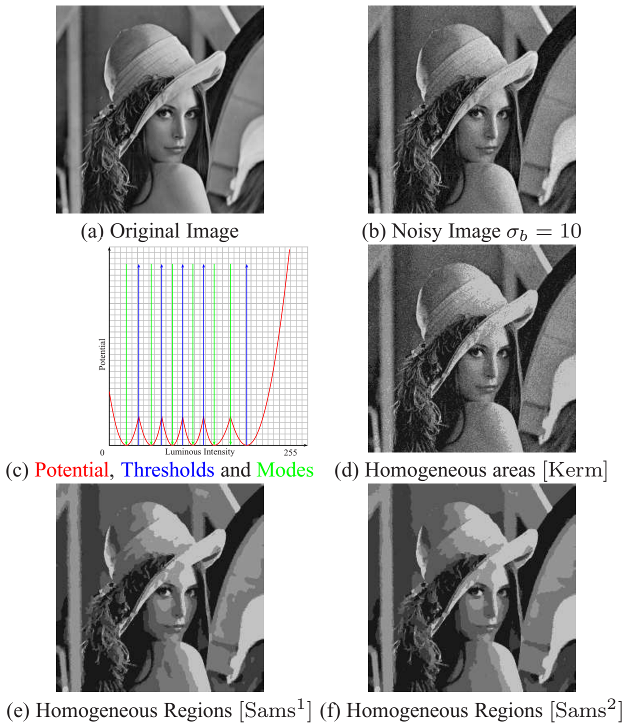

(a) Original Image

(b) Noisy Image $\sigma_b = 10$

(c) Potential, Thresholds and Modes

(d) Homogeneous areas [Kerm]

(e) Homogeneous Regions [Sams^1]

(f) Homogeneous Regions [Sams^2]

Fig. 2. Determination of the Homogeneous Areas of [LENA] degraded with an additive noise $\sigma_b = 10$